Design of a soil concrete as a new building material – Effect of clay and hemp proportions

Duc Chinh Ngo, Jacqueline Saliba, Nadia Saiyouri, Zoubir Medhi Sbartaï

DESIGN OF A SOIL CONCRETE AS A NEW BUILDING MATERIAL – EFFECT OF CLAY AND HEMP PROPORTIONS

Duc Chinh NGO[1,2], Jacqueline SALIBA[2], Nadia SAIYOURI[2], Zoubir Mehdi SBARTAÏ [2]

[1] University of Transport and Communications, 3 Cau Giay road, Dong Da district, Hanoi, Vietnam

[2]I2M, UMR 5295, Université de Bordeaux, 351 cours de la libération, 33405 Talence, France

Abstract

This study aims to optimize the composition of new ecological concrete constituted of upgraded excavated soil. The novelty of this study is the fact that earth concrete is poured with classical vibration as ordinary concrete. Several soil concrete mixtures, composed of different proportions of clayey soil, sandy soil and small amounts of cement, lime and hemp fibers have been tested. The mineralogical composition of clayey soil was studied by X-ray diffraction (XRD) analysis The chemical composition was established by Environmental Scanning Electron Microscopy (ESEM) coupled with the X-Ray Energy Dispersive Spectrometry (EDS). Casting of concrete mixtures has been realized by vibration, as ordinary concrete, to obtain the required workability on construction sites. Compressive tests have been carried out on samples at different curing times. Ultrasonic non-destructive technique has been used to monitor the hardening of soil concrete. As this concrete presents important volumetric changes that can cause the infiltration of water and impact their durability, an experimental investigation on autogenous and drying shrinkage is reported. Water porosity and water absorption tests have been also carried out to evaluate the transfer property of this porous material. The results show that the compressive strength of soil concrete is greater than 1 MPa, which is sufficient for filling application (wall of a frame building) and increases to 5 MPa after 6 months. Compressive strength, density, and workability of the tested concrete mixtures decrease with increasing clayey soil and hemp fibers. Desiccation shrinkage increases with the volume fraction of clayey soil and hemp fibers.

Keywords: Earth concrete, hemp fibers, mechanical and physical properties, ultrasonic monitoring, shrinkage.

1 Introduction

The ecological design of structures and sustainable development is nowadays of high importance in the construction industry. Thus, alternative building materials such as soil concrete containing a proportion of various ecological components are expected to be increasingly developed. The aim of producing ecological concrete is to reduce the consumption of cement and thus the CO_2 production, to provide an alternative to the scarcity of raw materials and to reduce the energy consumption in the production process. Recently, many changes have been observed in the construction methods with the aim to replace traditional concrete by alternative construction materials such as concrete containing a high proportion of various ecological components called "green" while maintaining acceptable properties for the desired application. The use of local materials is then strongly encouraged to minimize energy consumption [Kenai & al., 2014; Gonçalves & Martins., 2012]. For instance, constructions made of cost-effective raw soils are of real interest since their hydrothermal performance and acoustic properties are more important than that of ordinary concrete [Henri & Hugo, 2017, Palumbo & al., 2018]. However, more research is needed in order to have a better understanding of the mechanical properties and the durability of soil concrete.

Regarding the use of subgrade soil in concrete, it can be stabilized by using different kind of binders as lime and cement [Laborel-Préneron & al., 2016; Nalbantoglu & Tuncer, 2001; Rao & Shivananda, 2004; Tallah & al., 2016; Sariosseiri & Muhunthan, 2009; Makki-Szymkiewicz & al, 2015]. Soil-lime stabilization is due to the pozzolanic reaction where aluminous and siliceous minerals in clay react with lime to produce calcium silicates and aluminates that bond the particles together [Kumar & Gupta, 2016; Maubec & al., 2017]. The addition of cement increases the mechanical properties faster but can induce shrinkage and cracking [Kumar & Gupta, 2016; Costas, 2015]. Pozzolanic reactions are time and temperature dependent requiring longer hydration time with lime than cement [Eades & Grim, 1960]. Many studies showed that from 2% to 4% of lime, the Atterberg limits increase slightly, then stabilize and decrease when the amount of lime reaches 8% [Bell, 1996; Khattab & al, 2007; Al-

Mukhtar & al, 2014]. The increase of the rate of lime and cement increases the compressive strength [Bell, 1996; Costa, 2015]. The studies on lime modified soils showed that the optimal proportion of lime is about 3-6% in order to considerably modify the mechanical and the physical properties of the soil [Bell, 1996; Khattab & al., 2007; Al-Mukhtar & al, 2010]. Osinubi [Osinubi, 1998] and Nalbantoglu [Nalbantoglu & Tuncer, 2001] showed that the compressive strength and the permeability of soil strongly increase when the lime proportion is about 1-4%, while only a slight increase has been observed when the lime is between 3% and 7% of the total mass. Recently a hyper-compacted earth concrete was developed and showed interesting mechanical properties with compressive strength up to 30 MPa [Bruno et al, 2017].

In most of these studies, the modified soil is set up by compaction to produce a construction material. There is then a lack of knowledge regarding the use of soil in concrete having a minimum of workability to be casted with traditional vibration procedure. The originality of the proposed research study is that the formulated concrete has a good workability in order to be poured easily in formworks. The research of Hibouche [Hibouche, 2013] showed that, the treatment of soil with 8% of cement, 3% of lime and 0.4% of linen fibers allows the casting of a new soil concrete with interesting performances ($f_c \geq 0.5$ MPa) for filing application in building. Recently, [Ouellet-Plamondon & Habert, 2016] studied the rheological properties of self-compacted clay-based concrete and showed the potential of this material for the construction industry.

The addition of natural fibers as hemp fibers is particularly interesting as it minimizes the volume of waste in landfill. It is renewable and environmentally friendly [Zak & al., 2016; Khosrow & al., 1999]. Moreover, hemp fibers are naturally produced, and require almost no energy for their production and treatment. This makes hemp fibers concrete a carbon-negative construction material [Boutin & al., 2005; Saez-Perez & al., 2020]. Different binders can be used in hemp concrete [Sinka & al., 2018; Haik & al., 2020]. The addition of fibers can reduce the density, the shrinkage and cracking of concrete and improve the hygrothermal and acoustic properties in addition to its fire resistance [Makki-Szymkiewicz & al, 2015; Mostefai, 2015; Antonyova & al., 2017; Grubesa & al., 2018; Del Masto & al., 2019]. Kumar and Festugato [Kumar & Gupta, 2016; Festugato & al., 2017] showed that the addition of fibers reduces efficiently the development of tensile, shear cracks and soil

deformation. This is due to the bridge effect of fibers and load redistribution related to the increase of the total contact area between fibers and soil particles and consequently the friction between them [Taallah & Guettala, 2016]. A review of the properties and the different factors that affect the properties and the performance of hemp concrete can be found in [Jami & al., 2019; Saez-Perez & al., 2020]

Concrete volume change is an unavoidable phenomenon, from very early age to long-term behavior [Barcelo & al., 2001] and more particularly with soil concrete containing a high proportion of fines [Kanema & al., 2016; Omidi & al., 1996 a, b]. At early age, cementitious materials go through negative volumetric variations, due to chemical origins and thermal shrinkage linked to the hydration of the cement [Radocea, 1994]. The evaporation of water (drying shrinkage) and internal reactions (autogenous shrinkage) will result in the development of stresses within the liquid phase that leads to a volume reduction [Wang & al., 2001; Dias, 2003; Hover, 2006]. Autogenous shrinkage depends mainly on the composition of concrete and develops more rapidly with time than drying shrinkage [Audenaert & al., 2002; El-Dieb, 2007]. Drying shrinkage depends on the age of the beginning of drying and external parameters such as relative humidity and specimen size. If the tensile strength of concrete is lower than the stress level caused by movement restraint, cracking occurs [Hannant & al., 1999]. This cracking during shrinkage depends on the type of restraint, caused by the structure (externally applied restraint) and the material (internal restraint). Therefore, soil concrete structures are vulnerable to self-stresses or shrinkage cracking which may reduce their serviceability and durability. Thus, the understanding of shrinkage process and more particularly drying shrinkage, known as the main cause of micro and macro cracking, is essential.

In this study, soil concrete, which can be set up by vibration as traditional concrete, has been developed by incorporating optimal proportions of cement, lime and hemp fibers. Due to the variability of the available soils, an experimental investigation is proposed to study the effect of the proportion of clayey soil and hemp fibers on the mechanical and physical characteristics of the designed concrete.

2 Experimental program

2.1 *Materials and test methods*

Five different materials were used i.e. clayey soil, sandy soil, cement, lime, and hemp fibers. Cement and lime were added to stabilize the soil and to increase the compressive strength. The soils used in this study were obtained from two local construction sites and are classified according to the Unified Soil Classification System (USCS). The distribution of coarse particles was determined by sieve analysis while the distribution of fine particles was analyzed with the sedimentation method.

2.1.1. Clayey soil

Clayey soil is characterized in laboratory. Table 1 presents the results obtained by granulometric and sedimentation methods, Atterberg limits and methylene blue tests. They clearly indicate that the soil is "clayey with low plasticity" (I_p = 21.66 and W_l = 51.74%).

The clayey soil mineralogy was also studied by X-ray diffraction (XRD) analysis [Smith & al., 2001]. XRD patterns were obtained using a PANalitycal PW3020 Bragg-Brentano θ-2θ geometry diffractometer equipped with a secondary monochromator over an angular range 2θ=3°-80°.

Figure 1 shows the XRD patterns. The obtained peaks were identified using embedded database under EVA processing software. The diffractogram illustrates that the main minerals are: palygorskite, calcite, muscovite, goethite and dominated mainly by quartz.

The Environmental Scanning Electron Microscopy (ESEM) coupled with the X-Ray Energy Dispersive Spectrometry (EDS) was also used to observe the microstructure and complete the chemical composition of clayey soil. Figure 2 shows the ESEM images and the corresponding X-Ray EDS chemical maps. Figure 2a and 2b show a high magnification image of clayey soil while Figure 2c shows low magnification BSE image indicating a granular arrangement. The phase spectrum of the sample is presented in Figure 2d. The mineralogical interpretation of the phase spectrum reveals that it is dominated by quartz, muscovite and goethite.

2.1.2. Sandy soil

The main characteristics of the studied sandy soil are presented in Table 2. It is characterized by medium fineness of 2.33 and about 72% of sand. The grain size distribution of clayey and sandy soils is shown in Figure 3.

2.1.3. Hemp fibers

In this study, hemp fibers are used as a reinforcement material. Those fibers are one of the most natural common fibers and low-cost in France. Hemp fibers stem is constituted of a woody core with a hollow open sponge structure surrounded by bast fibers and are categorized as vegetal granulates. Their lengths vary between 5 and 25 mm with diameters less than 2 mm. Hemp fibers density is about 100 kg/m^3 in ambient condition [Del Masto & al. 2019]. The thermal conductivity is equal to λ = 0.05 W/m.K. Hemp fibers are highly hydrophilic and can absorb water up to 2.5 times of their weight.

2.1.4. Lime

The non-hydraulic lime (100 NHL5) from Saint Astier product (France), chosen in accordance with the European standard EN 459-1, is added to the tested concrete mixtures.

2.1.5. Cement

The cement CEM V (SV) 42.5 N is chosen based on two different principal criteria (clinker ratio and CO_2 impact). The main components and the mechanical properties of the cement are presented in Tables 3 and 4.

2.2 *Composition of the tested concrete*

A series of laboratory tests have been conducted on different soil concrete mixtures in order to study the possibility of increasing the clay proportion considering a mix design. Percentage of clayey soil was varied between 0% and 40% (0A, 20A, 30A, 40A) while the volume fraction of hemp fibers was modified from 0% to 1.2% (0F, 0.6F, 1.2F) for the 12 studied mixtures presented in Table 5.

The slump of these mixtures varies between 6.5 cm and 16.5 cm according to the percentage of clayey soil and hemp fibers. As the percentage of water is kept constant, soil concrete molding was more difficult with increasing the percentage of clayey soil and hemp fibers. For this reason, water content was increased to keep acceptable workability for construction industry (slumps > 6 cm).

2.3 *Specimens dimensions and preparation*

Dry components, as shown in Figure 4a, were first introduced in a blender (cement, lime, soil, and hemp fibers) and mixed for 5 minutes in order to obtain a homogeneous mixture. Water was then progressively added to ensure the mixing homogenization (Figure 4b). Slump test was conducted just after mixing to ensure a good workability with at least a slump of 7 cm.

Concrete was then poured in cubic molds with dimensions of 10×10×10 cm^3 (Figure 4c) in two layers. Each layer was compacted with a vibrating needle as an ordinary concrete. At least three samples were casted as replicates for each mix. Note here that the oversized gravels (higher than 10 mm) have been removed from the used soil to ensure a good workability. Specimens are conserved under sealed conditions by covering them with a plastic sheet to prevent the drying of earth concrete. After 24h, specimens were removed from the molds and conserved in a plastic box under a temperature of 20°C and a relative humidity between 90% and 100%, without direct contact between water and specimens.

2.4 *Compressive tests*

The unconfined compressive tests have been carried out by using an electromechanical machine having a capacity of 50 kN. The loading of concrete has been applied with a steel plate at a constant rate of 0.5 mm/min by means of jack displacement. Specimens have been equipped with two sensors to measure the vertical displacement and two sensors for horizontal displacements (Figure 4d).

2.5 *Three-point bending test*

Three-point bending fracture tests were also achieved on soil concrete beams with the dimensions of 100×150×600 mm^3 (L×h×b) and an effective span (S) equal to 500 mm. The fracture test uses a load-

controlled universal testing machine as per RILEM-TMC 50 recommendations [RILEM, 1985]. Tests were conducted using an electromechanical machine with a capacity of 100 kN under closed-loop crack opening displacement (CMOD) control with two LVDT sensors placed at the bottom of the beam (Figure 5). The load was applied with a crack opening displacement rate of 0.2 mm/min.

2.6 *Measurement of the ultrasonic pulse velocity*

A movable system composed of a pulse generator PUNDIT (Portable Ultrasonic Nondestructive Digital Indicating Tester) with a direct transmission mode was used (Figure 6). A pulse of ultrasonic longitudinal stress waves with a frequency of 200 kHz is introduced into one surface of the concrete by a transducer coupled to the surface with a coupling gel. The pulse travels through the concrete and is received by a similar transducer coupled on the opposite surface. The propagation velocity is calculated using the relation in equation 1. Before each measurement, the device was calibrated according to the test procedure presented in figure 6.

$$V = \frac{L}{t} \text{ (m/s)} \qquad Eq.1$$

Where t is the propagation time and L the propagation distance.

2.7 *Durability tests*

The durability of earth concrete is closely related to the porosity and more particularly to the fluid penetration and moving through the material. Thus, controlling the processes of drying and wetting of concrete is of main importance in order to understand degradations, which can occur with time.

2.7.1 Water porosity measurement

The porosity can be used as an indicator of the durability of concrete. Thus, water porosity measurements have been carried out and correlated with concrete properties as the compressive strength and the corresponding effect of clayey soil and fibers. Two specimens with dimensions of 5×5×5 cm^3 were used for each mix at 28 days. Specimens were first dried to constant weight in ventilated oven at 60°C. Specimens were then placed in a hermetic glass bell under a low pressure of one bar of vacuum during 24 h. Then, the bell was filled with water and the specimens kept under

vacuum with low pressure for 24 hours to equilibrate and ensure full saturation of specimens. The weights of specimens were then measured in air and water. Porosity P (%) was calculated as follows:

$$P = \frac{m_{sat} - m_{dry}}{m_{sat} - m_{sat}^{sub}} \times 100\ (\%) \qquad Eq.2$$

where:

m_{dry} : oven-dry weight of specimen.

m_{sat} : saturated weight of specimen (weighed in air)

m_{sat}^{sub}: saturated submerged weight of specimen (weighed in water)

The bulk density ρ_{app} (kg/m^3) is also calculated as :

$$\rho_{app} = \frac{m_{dry} * \rho_{wat}}{m_{sat} - m_{sat}^{sub}}\ (\text{kg.m}^{-3}) \qquad Eq.3$$

Where ρ_{wat} is the water density (1000 kg/m^3).

2.7.2 Capillarity absorption measurement

The capillary water absorption was measured according to the AFNOR standard XP P 13-901 (AFNOR-XP P13-901). Specimens with dimensions of 10×10×10 cm^3 have been used for each mix at 28 days. Specimens were first dried to constant weight in oven at 60°C. Then, the specimens were immersed in a thin layer of water (10 mm) and the mass of specimens was continuously measured (Figure 7).

The water absorption coefficient is calculated according to the following formula:

$$C_b = \frac{100 * (P_1 - P_0)}{S\sqrt{t}}\ (\text{g/cm}^2\text{min}^{1/2}) \qquad Eq.4$$

Where:

C_b: capillary coefficient

P_1: Weight of the specimen after immersion in water (g)

P_0: Weight of the specimen before immersion in water (g)

S: Submerged surface of the specimen (cm^2)

t: Water immersion time of the specimen (min)

2.8 *Shrinkage and water loss measurement tests*

Soil concrete specimens were prepared with prismatic molds of 4x4x16 cm^3. Specimens were covered with a thin sheet of plastic to prevent water loss and maintained at 20°C during 24 h. Then, specimens were unmolded and shrinkage measurements were performed on drying and sealed specimens (Figure 8a). For this latter, the exchange of moisture was prevented by covering specimens with a double layer of self-adhesive aluminum paper. Shrinkage tests were performed in a controlled climate chamber at 60% of RH and a temperature of 20°C.

For drying shrinkage, specimens were not covered on lateral sides, except for the top surfaces, in order to create a one-dimensional drying. Shrinkage of hardened soil concrete was measured with a device equipped with an LVDT sensor (Figure 8b), which allows following the length of the specimen. Weight loss was simultaneously measured in parallel for a better comprehension of shrinkage phenomenon.

3 Results and discussions

3.1 *Compressive test results*

Three specimens have been tested for each mixture and the mean value and the standard deviation have been calculated. The uniaxial compressive strength of the tested specimens, with free lateral expansion, is defined as the ratio of the axial ultimate force to the cross-section. Figure 9 shows typical curves of the compressive strength versus the vertical and horizontal strain at 7 days, 28 days, and 180 days for the mixture N°12 (40% of clayey soil and 1.2% of hemp fibers). The results show that the mechanical properties (compressive strength and Young modulus) increase significatively even after 28 days, on the contrary to ordinary concrete. After 180 days, compressive strength reaches values more than twice that measured at 28 days. The elastic modulus increases from 2 GPa at 7 days to 8 GPa at 180 days. After the maximum loading, mechanical behavior of the material is less ductile with respect to curing time. This strength increase, after a long curing, is related to the formation of hydration products as the CSH and ettringite due to the presence of cement and lime in addition to the carbonation that may be responsible of a denser structure [Balciunas & al., 2018].

Figures 10 to 12 show the effect of clayey soil and hemp fibers on the compressive strength at 7, 28, and 180 days respectively when specimens were cured under controlled relative humidity (20°C and 90-100% RH). The standard deviation of the results is less than 0.025 MPa, which is of about 4% at 7 days. This variability is due to the heterogeneity of sandy and clayey soil and to the multi-scale porous structure [Collet & al. 2008].

The results show that the compressive strength decreases slightly with the addition of clayey soil at 7 days and varies between 0.6 and 1.2 MPa (Figure 11). The compressive strength varies between 1 and 2.4 MPa at 28 days and between 2.5 and 5 MPa at 180 days (Figure 11, and 12). However, the effect of clay proportion on compressive strength is small (less than 0.3 MPa) when clayey soil volume fraction varies from 20 to 40%. This effect is not significant when the compressive strength is stabilized at 180 days.

The addition of fibers in soil concrete with 0% of clayey soil decreases the compressive strength at 7, 28 and 180 days. This effect is more significant at 28 and 180 days (about 0.8 MPa of variation). However, with the addition of clayey soil, the effect of fibers shows low variations. A significant effect can be only observed for 1.2% of fiber at 28 and 180 days in which the compressive strength decreases of about 0.5 MPa. This negative effect of fibers on the compressive strength may be due to the lower density, the change of the soil concrete structure, the intergranular void and pore distribution by introducing voids and discontinuity [Awwad & al., 2012]. The addition of fibers as reinforcement in soil concrete specimens can hinder the lateral strain during compressive loading [Hannawi & al., 2016], which can explain the observed ductility on the stress-strain curves of soil concrete with fibers. In addition, fibers can be responsible of the increase of the friction angle at the shear cracking surface [Chabannes & al., 2017].

The effect of the curing time of soil concrete on the compressive strength has also been studied. Figure 13 shows the evolution of the compressive strength for the different mixtures at 7, 28, and 180 days. The results show that the compressive strength increases even after one month. This is an important property of this concrete compared to traditional concrete. The short-term compressive strength is mainly associated to cement hydration, while the long-term compressive strength may be provided by the hydration reaction, the pozzolanic reactions between clay minerals and calcium

hydroxide formed by cement hydration [Si Ho & al., 2017]. In addition, a part of water is stored in claim which leads to the hydration of cement even after 28 days as long as water is available.

The measured compressive strength of soil concrete is low (from 1 to 2.4 MPa at 28 days) compared to ordinary concrete. However, these strengths are acceptable regarding the application of this kind of concrete which is used as a filling concrete and not for assuring high load capacity (e.g. walls, Blocks, etc.) [Mazhoud & al., 2017]. This is due to the very low percentage of cement the higher porosity of soil concrete constituted of fine-grained mixtures and the higher water content required to achieve an acceptable workability. However, the acoustic and thermal properties could be better than traditional concrete due to the use of clayey soil and hemp fibers.

3.2 *Bending test*

The knowledge of tensile strength is important as tensile stresses can be generated by shrinkage, by seasonal variations in temperature, by alternate wetting and drying and by loading that can generate tensile and shear stress [Ozkul & Baykal, 2007]. Figure 14 shows the average load CMOD curves for soil concrete with respect to clayey soil proportion variation from 0 to 40 % and the percentage of fibers from 0 to 1.2%. The load-CMOD variations are linear up to about 80% of the ultimate load followed by a nonlinear variation up to the peak load. A stable failure was then observed in the post-peak region. The results show that the bending strength decreases largely with the addition of clayey soil. However, the addition of hemp fibers improves the fracture properties as the bending strength, the fracture energy and the ductility of soil concrete. This may be attributed to the good interfacial adhesion existing between the fibers and the matrix leading, at some load level, fibers bridging the crack to be activated in carrying tensile stresses and thus decreasing the crack propagation kinetic [Donkor & Obonyo, 2015; Iucolano & al., 2019].

3.3 *Monitoring of soil concrete by using the Ultrasonic method*

The Ultrasonic Pulse Velocity (UPV) of the mechanical P waves depends on the same parameters that influence the mechanical properties such as density, porosity, and elasticity of the material [Bungey & al., 2006; B.S., 1986]. Thus, the elasticity modulus and the compressive strength can be

329 determined based on the UPV values. The UPV is a non-destructive test that allows the monitoring of
330 concrete hardening and can be used to estimate the time of removing formworks, which can optimize
331 construction cost.
332 In this study, the UPV has been measured in order to study the effect of fibers and clayey soil on the
333 strengthening of the designed concrete mixtures with age. Cubic specimens with dimensions of
334 $10\times10\times10$ cm^3 have been tested during four months of curing (from 5 days until stabilization).
335 The UPV of specimens of all mixes increases during the curing period with an important rate during
336 the first days indicating that soil concrete develops mechanical strength at early age (Figure 15).
337 After one month, UPV continues to increase slightly.
338 The effect of the variation of the volume ratio of fibers on the UPV is illustrated in Figure 15 a, b, c
339 and d for 0%, 20%, 30%, and 40% of clayey soil, respectively. The addition of hemp fibers decreases
340 slightly the UPV due to the decrease of the density. This slight effect is also observed for
341 compressive strength, which confirms the UPV results. It can be also noted that the UPV decreases
342 with the increase of clayey soil ratio, which could be related to the increase of concrete porosity
343 [Mandal & al. 2016]. In addition, UPV increases with a more important rate and amplitude for soil
344 concrete with 0% of clayey soil in comparison with mixtures with 20%, 30%, and 40% where a slight
345 difference has been observed for compressive tests.
346 Figure 16 presents the correlation between the compressive strength and the corresponding UPV
347 values at 7, 28, and 180 days. An exponential function can be considered by a regression analysis.
348 This statistical regression analysis consisted in calculating the exponential function parameters by
349 using least mean squares method that minimizes the error between the proposed function
350 (exponential in this case) and the experimental measurements. The results are presented in Figure 16
351 with a coefficient of determination of about $R^2 = 0.75$ that indicates a good correlation. Then, the
352 UPV measurements can provide effective means to determine the mechanical properties of soil
353 concrete [Mandal & al., 2016]. The UPV can be then used for on-site monitoring of soil concrete in
354 order to control the compressive strength variations during construction.
355

3.4 *Shrinkage tests*

Figure 17 presents the evolution of autogenous and drying shrinkage versus time of soil concrete with 0%, 20%, 40% of clayey soil, and 0%, 1.2% of hemp fibers. The rate of autogenous shrinkage is important during the first three days and decreases gradually with time (Figure 17a). Autogenous shrinkage occurs independently of external water loss. It is a result of chemical shrinkage and self-drying shrinkage. The reduction in the relative humidity in the pore system causes water–air meniscus that subjects the pore walls to considerable stress and leads to substantial self-drying shrinkage. The results show that autogenous shrinkage of soil concrete without fibers increases with the proportion of clayey soil with values four times more important for the mixes with 40% of clayey soils. The addition of 1.2% of fibers shows a slight increase of autogenous shrinkage for the mixes with 0% and 20% of clayey soil. However, the addition of fibers decreases significantly the autogenous shrinkage of soil concrete with 40% of clayey soil. These differences are related to the variation of the global porosity between soil concrete mixes and the high water absorption of fibers [Fourmentin & al., 2016; Stevulova & al., 2015].

Figure 17b represents the drying shrinkage calculated as the subtraction of the autogenous shrinkage from the overall shrinkage. The rate of drying shrinkage increases quickly at the beginning to stabilize between 10 and 15 days.

Drying shrinkage deformation increases with the rate of clayey soil and reaches important values for soil concrete with 40% of clayey soil (6 times higher than that with 0% of clayey soil). The addition of 1.2% of fibers influences slightly the amplitude of the shrinkage with 0% and 20% of clayey soil, however it decreases the amplitude of drying shrinkage for the mix having 40% of clayey soil with an important rate.

Water weight loss is also measured during drying shrinkage and presented in Figure 18a. The variation of water weight loss transcribes the diffusion capacity of the material. The weight loss is important during the first 15 days. The water weight loss shows the same tendency as drying shrinkage. The water weight loss increases with the proportion of clayey soil, which could explain the increase of drying shrinkage. The addition of fibers increases the water weight loss for soil concrete with 0% and 20% of clayey soil while it decreases the water weight loss for soil concrete

with 40% of clayey soil. The water weight loss shows a good correlation with the amplitude of shrinkage. Thus, the evolution of the drying shrinkage is also plotted as a function of the weight loss (Figure 18b). Two phases can be distinguished, during the first phase called sleeping zone, the gradient of water content due to drying generates a stress gradient and thus a high tension in the skin layer and cracking. The surface area to volume ratio is an important factor in this phase. During the second phase, gradients become more pronounced and the cracking in the skin remains unchanged and shrinkage is proportional to drying (linear zone). Soil concrete shrinkage is very high in comparison with ordinary concrete due to the absence of large aggregate that restrain the overall shrinkage and to the higher porosity related to the incorporation of clayey soil and the high water content.

3.5 *Durability tests: water porosity and water absorption*

Figure 19a presents the evolution of the bulk density versus the clayey soil proportion and hemp fibers at 7 and 28 days. The results show that the increase of the percentage of clayey soil and fibers decreases the bulk density. The bulk density is about 1763 kg/m^3 for soil concrete with 0% of clayey soil and decreases to 1534 kg/ m^3 with the addition of 1.2% of hemp fibers at 28 days. In addition, the bulk density increases with age due to different hardening mechanisms as cement hydration. These values are in accordance with those obtained in the literature and indicate the potential of hemp fibers and clayey soil to reduce the thermal conductivity of concrete [Taallah & Guettala. 2016].

Figure 19b describes the correlation between the compressive strength and porosity at 7 days and 28 days. An exponential regression equation is fitted to the data in accordance with the literature for porous material [Lian & al., 2011]. As expected, the compressive strength decreases with mixtures of higher porosity. In fact, as the density decreases, the number of contact points, responsible for transmitting stress, decreases leading to the decrease of the compressive strength.

Capillarity absorption measurements were conducted in order to study the ability of the material to absorb water. The capillary suction through the pores system can be then used as an indicator of the open porosity. Figure 20a represents the water absorption coefficient for soil concrete with various fibers and clayey soil content. The results show that the addition of clayey soil and hemp fibers

412 increases the capillary absorption. The kinetic of water absorption is related to the kinetic of filling
413 pores with water shown by a stabilization of weight specimens. This kinetic depends on complex
414 phenomenon related to the connectivity between the pores where water may be transferred through
415 the multiscale micro porosity in the matrix, at the interface between the matrix and the fibers or even
416 in the cell structure of hemp fibers [Colinart & al., 2020]. Figure 20b shows that the water absorption
417 coefficient (calculated at 6 hours) is between 8.2 and 14.3 for soil concrete without fibers, while the
418 water absorption coefficient for soil concrete with fibers varies from 11.4 to 15.2. This can be
419 explained by the increased voids created in the mixture due to the existence of fibers and clay and
420 their hydrophilous behavior [Khiari & al., 2010, Shafiei & al., 2010; Pejic & al., 2008]. Similar
421 values have been obtained by [Colinart & al., 2020].

422 **4 Conclusions**

423 The development of a new environmentally friendly construction material has been realized in this
424 study using local soil as a principal component. The effect of clayey soil and hemp fibers on the
425 mechanical properties of soil concrete have been studied. Twelve concrete mixtures with different
426 percentages of clayey soil and hemp fibers have been tested under controlled relative humidity.

427 The results show that the compressive strength of the tested concrete decreases with increasing the
428 proportion of hemp fibers and clayey soil which could be related to the increase of the porosity of soil
429 concrete. The slight negative effect of fibers on the compressive strength may be also due to the
430 lower density and the change of the soil concrete structure and pore distribution by introducing voids
431 and discontinuity. In addition, the compressive strength continues to increase even after one month
432 with values two times higher than that measured at 28 days. The measured compressive strength
433 varies from 1 MPa to 5 MPa with slump higher than 6.5 cm depending on the curing condition, the
434 clayey soil, and hemp fibers proportions. The UPV decreases with the addition of clayey soil and
435 hemp fibers showing a good correlation with the compressive strength.

436 Autogenous shrinkage increases with the increase of the proportion of clayey soil. Drying shrinkage
437 increases with the rate of clayey soil and reaches important values for soil concrete with 40% of
438 clayey soil (5 to 6 times higher than that with 0% of clayey soil). The addition of 1.2% of fibers

439 influences slightly the amplitude of shrinkage with 0% and 20% of clayey soil. However, it increases
440 the amplitude of drying shrinkage for the mix having 40% of clayey soil with an important rate due to
441 the change in the porosity that modifies the evaporation rate and consequently the rate of shrinkage.
442 Durability tests indicate that the porosity and water absorption increase with increasing soil
443 proportions. The incorporation of hemp fiber for density reduction and improving the thermal and
444 acoustic properties leads to an increase of the water absorption of about 9% for concrete with 20% of
445 clayey soil.
446 The generalization of this study may have a limitation since a specific clayey soil has been used
447 without the incorporation of additives. Additional studies should be done in order to evaluate the
448 effect of clay mineralogy and other additions, such as water reducer plasticizer, on the mechanical
449 and physical properties of earth concrete. Tests are currently investigated in order to study the
450 dimensional stability of soil concrete regarding shrinkage at early age, creep and
451 humidification/drying cycles.
452
453
454
455

5 References

Del Masto A., Trivaudey F., Guicheret-Retel V., Placet V., Boubakar L. 2019. Investigation of the possible origins of the differences in mechanical properties of hemp and flax fibres: A numerical study based on sensitivity analysis. Composites Part A: Applied Science and Manufacturing. Vol.4

AFNOR–XP P13–901: Compressed earth blocks for walls and partitions : definitions - specifications - test methods - delivery acceptance conditions.

Al-Mukhtar M. Lasledj A. Alcover J.F. 2010. Behaviour and mineralogy changes in lime-treated expansive soil at 20 °C. Applied Clay Science 50 : 191–198.

Al-Mukhtar M. Lasledj A. Alcover J.F. 2014. Lime consumption of different clayey soils. Applied Clay Science 95 133–145.

Amziane S., Sonebi M. Overview on bio-based building material made with plant aggregate, 2016. RILEM Technical Letters. Vol 1: 31 – 38.

Antonyová A., Antony P., Korjenic A., 2017. Evaluation the hygrothermal effects of integration the vegetation into the building envelope. Energy and Buildings. Vol. 136 : 121–138.

Audenaert K., De-Schutter G., 2002. Towards a fundamental evaluation of water retention tests for curing compounds. Mater. Struct. 35 (August) : 408 – 14.

Awwad E., Mabsout M., Hamad B., Talal Farran M., Khatib H., 2012. Studies on fiber-reinforced concrete using industrial hemp fibers. Construction and Building Materials. Vol. 35 : 710–717

B.S.. 1986. Testing concrete – recommendations for measurement of velocity of ultrasonic pulses in concrete. British standards institution. 1881 – 203. P. 24.

Balciunas G., Pundiene I., Boris R., Kairyte A., Zvironaite J., Gargasas J., 2018. Long-term curing impact on properties, mineral composition and microstructure of hemp shive-cement composite. Construction and Building Materials. Vol. 188 : 326–336

Barcelo L., Boivin S., Acker P., Toupin J., Clavaud B., 2001. Early age shrinkage of concrete: Back to physical mechanisms. Concr. Sci. Eng. 3 (10) : 85 – 91.

Bell F.G. 1996. Lime stabilization of clay minerals and soil. Eng. Geol. Vol. 42 (4) : 223 – 237.

Boutin M.P., Flamin C., Quinton S., Gosse G., 2005. Analysis of life cycle of 1. Thermoplastic compounds loaded with hemp fibers, and 2. Hemp concrete wall on wood structure. French Ministry of Agriculture – INRA report MAP 04 B1 05 01 (in French).

Bruno W A., Gallipoli D., Perlot C., Mendes J., 2017. Mechanical behaviour of hypercompacted earth for building construction. Materials and Structures, 50:160.

Bungey J.H., Millard S.G. Grantham M., 2006. Testing of concrete in structures. Fourth ed. Taylor & Francis. 353 p.

Chabannes M., Becquart F., Garcia-Diaz E., Abriak N.-E., Clerc L., 2017. Experimental investigation of the shear behaviour of hemp and rice husk-based concretes using triaxial compression. Construction and Building Materials. Vol. 143 : 621–632

Colinart T., Vinceslas T., Lenormand H., Hellouin De Menibus A., Hamard E., Lecompte T., 2020. Hygrothermal properties of light-earth building materials. Journal of Building Engineering. Vol. 29.

Collet F., Bart M., Serres L., Miriel J., 2008. Porous structure and water vapor sorption of hemp-based materials. Constr. Build. Mater. 22: 1271 – 1280.

Costas A. 2015. Strength properties of an epoxy resin and cement-stabilized silty clay soil. Applied Clay Science 114 : 517–529

Dias WPS., 2003. Influence of mix and environment on plastic shrinkage cracking. Mag. Concr. Res. 55 (4) : 385 – 94.

Donkor P., Obonyo E., 2015. Earthen construction materials: assessing the feasibility of improving strength and deformability of compressed earth blocks using polypropylene fibers. Materials & Design. 83: 813-819.

Eades J.L. Grim R.E. 1960. Reaction of hydrated lime with pure clay minerals in soil stabilization. Highway research board bulletin. 262: 51 – 53.

El-Dieb A.S., 2007. Self-curing concrete: water retention, hydration and moisture transport. Constr. Build. Mater. 21: 1282 – 7.

Festugato L., Menger E., Benezra F., André K. E., 2017. Fiber – reinforced cement soils compressive and tensile strength assessment as a function of filament length. Geotext. Geomembr, Vol. 45 : 77 – 82.

Fourmentin M., Faure P., Pelupessy P., Sarou-Kanian V., Peter U., Lesueur D., Rodts S., Daviller D., Coussot P., 2016. NMR and MRI observation of water absorption/uptake in hemp shives used for hemp concrete. Constr. Build. Mater. 124 : 405 – 413.

Gonçalves A., Martins I. Sustainability of construction materials-An overview, 2012. CDS12-International conference Durable Structures: from construction to rehabilitation, Lisbon, Portugal.

Grubeša I. N., Markovic B., Gojevic A., Brdaric J., 2018. Effect of hemp fibers on fire resistance of concrete. Construction and Building Materials. Vol. 184 : 473–484Haik R., Bar-Nes G., Peled A., Meir I.A., 2020. Alternative unfired binders as lime replacement in hemp concrete. Construction and Building Materials. Vol. 241.

519 Hannant D.J., Branch J., Mulheron M., 1999. Equipment for tensile testing of fresh concrete. Mag.
520 Concr. Res. 51 (4) : 263 – 7.

521 Hannawi K., Bian H., Prince-Agbodjan W., Raghavan B., 2016. Effect of different types of fibers on
522 the microstructure and the mechanical behavior of ultra-high performance fiber-reinforced concretes.
523 Compos. Part B 86 : 214 – 220.

524 Henri V. D. Hugo H. 2017. Earth concrete. Stabilization revisited. Cement and Concrete Research.

525 Hibouche A., 2013. Sols traités aux liants : Performances hydro - mécaniques et hygro - thermiques.
526 Applications en BTP. Ph.D thesis, Université du Havre, 374 p.

527 Hover KC., 2006. Evaporation of water from concrete surface. ACI Mater J. 103 (5): 384 – 9.

528 Iucolano F., Boccarusso L., Langella A., 2019. Hemp as eco-friendly substitute of glass fibres for
529 gypsum reinforcement: Impact and flexural behaviour. Composites Part B. Vol. 175.

530 Jami T., Karade S.R., Singh L.P., 2019. A review of the properties of hemp concrete for green
531 building applications. Journal of Cleaner Production. Vol. 239.

532 Kanema J.M., Eid J., Taibi S., 2016. Shrinkage of earth concrete amended with recycled aggregates
533 and superplasticizer: impact on mechanical properties and cracks. Materials and Design 109:378-389.

534 Kenai S, Menadi B, and Khatib J.M., 2014. Low carbon building materials for sustainable
535 construction. ACEM, Busan, Korea august 24-28.

536 Khattab S.A.A. Al-Mukhtar M. Fleureau J.M. (2007): Long–term characteristics of a lime treated
537 plastic soil. Journal of Materials in Civil Engineering. vol. 19. n° 4. pp 358 – 366.

538 Khiari R., Mhenni M.F., Belgacem M.N., Mauret E., 2010. Chemical composition and pulping of
539 date palm rachis and Posidonia oceanica – a comparison with other wood and non-wood fibre
540 sources, Bioresour. Technol. 101 (2) : 775 – 780.

541 Khosrow G., Romildo D., Toledo F., 1999. Behavior of composite soil reinforced with natural fibers.
542 Cem. Concr. Compos. 21 (1), 39 – 48.

543 Kumar A., Gupta D., 2016. Behavior of cement – stabilized fiber – reinforced pond ash, rice husk ash
544 – soil mixtures, Geotext. Geomembr. Vol. 44 : 466 – 474.

545 Laborel-Préneron A. Aubert J.E. Magniont C. Tribout C. Bertron A. 2016. Plant aggregates and
546 fibers in earth construction materials. A review. Const. Build. Mater. Vol.111 : 719 – 734.

547 Lian C., Zhuge Y., Beecham S., 2011. The relationship between porosity and strength for porous
548 concrete. Construction and Building Materials. vol. 25 : 4294 – 4298.

549 Saez-Perez M.P., Brümmer M., Duran-Suarez J.A., 2020. A review of the factors affecting the
550 properties and performance of hemp aggregate concretes. Journal of Building Engineering. Vol. 31

551 Makki-Szymkiewicz L., Hibouche A., Taibi S., Herrier G., Lesueur D., Fleureau J., 2015. Evolution
552 of the properties of lime-treated silty soil in a small experimental embankment. Engineering Geology
553 191 (2015) 8–22.

554 Mandal T. Tinjum J.M. Edil T.B. 2016. Non-destructive testing of cementitiously stabilized materials
555 using ultrasonic pulse velocity test. Transportation Geotechnics. Vol. 6: 97-107.

556 Maubec N. Deneele D. Ouvrard G. 2017. Influence of the clay type on the strength evolution of lime
557 treated material. Applied Clay Science .137 : 107–114.

558 Mazhoud B., Collet F., Pretot S., Lanos C., 2017. Mechanical properties of hemp-clay and hemp
559 stabilized clay composites. Construction and Building Materials. Vol. 155 : 1126–1137

560 Mostefai N., Hamzaoui R., Guessasma S., Aw A., Nouri H., 2015. Microstructure and mechanical
561 performance of modified hemp fibre and shiv mortars: Discovering the optimal formulation.
562 Materials and design. Vol. 84 : 359-371.

563 Nalbantoglu Z. Tuncer E. R. 2001. Compressibility and hydraulic conductivity of a chemically
564 treated expansive clay. Canadian Geotechnical Journal. Vol. 38. 7 :154 – 160.

565 Omidi G.H., Prasad T.V., Thomas J.C., Brown K.W., 1996a. Influence of amendments on the
566 volumetric shrinkage and integrity of compacted clay soils used in landfill liners. Water Air Soil
567 Pollut. 86 : 263 – 274.

568 Omidi G.H., Thomas J.C., Brown K.W., 1996b. Effect of drying cracking on the hydraulic
569 conductivity of a compacted clay liner. Water Air Soil Pollut. 89 : 91 – 103.

570 Osinubi K. J. 1998. Permeability of lime-treated lateritic soil. Journal of Transportation
571 Engineering. 124(5) : 465 – 469.

572 Ouellet-Plamondon CM., Habert G, 2016. Self-Compacted Clay based Concrete (SCCC): proof-of-
573 concept. Journal of Cleaner Production. Vol 117:160-168.

574 Ozkul Z.H., Baykal G., 2007. Shear behavior of compacted rubber fiber-clay composite in drained
575 and undrained loading. ASCE J. Geotech. Geoenviron. 7, 767 – 781.

576 Palumbo M., Lacasta A.M., Giraldo M.P., Haurie L., Correal E., 2018. Bio-based insulation materials
577 and their hygrothermal performance in a building envelope system (ETICS). Energy & Buildings.
578 Vol. 174 : 147–155.

579 Pejic B. M., Mirjana K. M., Petar D., Jovana P. Z., 2008. The effects of hemicelluloses and lignin
580 removal on water uptake behavior of hemp fibers. Bioresour. Technol. 99 : 7152 – 7159.

581 Radocea A., 1994. A model of plastic shrinkage. Mag. Concr. Res. 46 (167) : 125 – 32.

582 Rao S. M. Shivananda P. 2004. Compressibility behavior of lime-stabilized clay. Geotext. 23: 309 –
583 319.

584 RILEM 50-FMC Recommendation (1985). Determination of fracture energy of mortar and concrete
585 by means of three-point bend test on notched beams. Materials and Structures. 18:285-290.

586 Sariosseiri F. Muhunthan B. 2009. Effect of cement treatment on geotechnical properties of some
587 Washington State soils. Eng. Geol. 104. 119 –125.

588 Shafiei M., K Karimi., Taherzadeh M.J., 2010. Palm date fibers: analysis and enzymatic hydrolysis,
589 Int. J. Mol. Sci. 11 : 4285–4296.

590 Si Ho L., Nakarai K., Ogawa Y., Sasaki T., Morioka M., 2017. Strength development of cement-
591 treated soils: effect of water content. carbonation and pozzolanic reaction under drying curing
592 condition. Const. Build. Mater. Vol.134 : 703 - 712.

593 Sinka M., Van den Heede P., De Belie N., Bajare D., Sahmenko G., Korjakins A., 2018. Comparative
594 life cycle assessment of magnesium binders as an alternative for hemp concrete. Resources,
595 Conservation & Recycling. Vol. 133 : 288–299.

596 Smith, D.K., Johnson, G.G., Ruud, J. and Clayton, O. (2001) Clay Mineral Analysis by Automated
597 Powder Diffraction Analysis Using the Whole Diffraction Pattern. Powder Diffraction, 16, 181-185.

598 Stevulova M., Cigasova N., Purcz J., Schwarzova P., 2015. Long-Term water absorption behavior of
599 hemp hurds composites. Mater. 8 : 2243 – 2257.

600 Taallah B., Guettala A., 2016. The mechanical and physical properties of compressed earth block
601 stabilized with lime and filled with untreated and alkali-treated date palm fibers. Constr.Build. Mater.
602 Vol. 104 : 52 – 62.

603 Wang K., Shah SP., Phuaksuk P., 2001. Plastic shrinkage cracking in concrete materials-influence of
604 fly ash and binders. ACI Mater J. 98 (6) : 458 – 64.

605 Zak P., Ashour T., Korjenic A., Korjenic S., Wu W., 2016. The influence of natural reinforcement
606 fibers, gypsum and cement on compressive strength of earth bricks materials. Const. Build. Mater.
607 Vol. 106 : 179 – 188.

608

609

610

611

612

613

List of tables

List of figures

651 **TABLES**

652

653 **Table 1: Characteristics of clayey soil**
654

Test	Criterion	Value (%)	USCS
Atterberg limits	Liquid limit W_L	51.74	Clayey with low plasticity (CL)
	Plastic limit W_P	30.08	
	Plasticity index I_P	21.66	
Sedimentation and Granulometric tests	Clay (< 0,002 mm)	25.06	
	Silt (0,002 – 0,06 mm)	55.94	
	Sand (0,06 – 2 mm)	19	
	Gravel (>2 mm)	0	
Methylene Blue test	VBS	5.72	Clayey silty soil

655
656
657 **Table 2: Characteristics of sandy soil**
658

Test	Criterion	Value (%)	USCS
Granulometric	Silt (0,002 – 0,06 mm)	0.64	Sandy soil
	Sand (0,06 – 2 mm)	72.54	
	Gravel (> 2 mm)	26.82	
Blue methylene	VBS	0.67	
Specific density (kg/m^3)		2.33	
Fineness modulus		2.57	SP Poorly graded sands, gravelly sands, low fines
C_U		4.38	
C_C		2.28	
Sand equivalent			
Visual		78.44	
With the piston		76.32	

659
660
661 **Table 3: Mineralogical composition of cement**
662

Type of cement	Main components (% by weight)			Secondary component
	Clinker Portland	Blast furnace cinder	Fly ash	
CEM V/A (S-V)	40 - 64	18 – 30	18 - 30	0 - 5

663
664
665

Table 4: Compressive strength of cement

Resistance class	Compressive strength (MPa)				Time of setting (min.)
	Short-term strength		strength at		
	2 days	7 days	28 days		
42,5 N	≥ 10,0	-	≥ 42,5	≤ 62,5	≥ 60

Table 5: Proportions of the different soil concrete mixtures

N°	Mixes	Clayey soil (kg/m^3)	Sandy soil (kg/m^3)	Cement (kg/m^3)	Lime (kg/m^3)	Fibers (kg/m^3)	Water (kg/m^3)	Slump (cm)
1	0A0F	0.00	1386.8	151.8	45.0	0.0	330.6	16.5
2	0A0.6F	0.00	1306.2	144.3	42.8	12.0	314.2	16.2
3	0A1.2F	0.00	1238.2	138.0	40.9	22.9	300.6	15.7
4	20A0F	247.8	991.4	135.6	40.2	0.0	398.9	10.5
5	20A0.6F	241.4	965.7	133.3	39.5	11.1	392.1	14.8
6	20A1.2F	236.6	946.7	131.9	39.1	21.9	388.0	9.5
7	30A0F	368.3	859.5	134.4	39.9	0.0	417.6	9.5
8	30A0.6F	356.3	831.5	131.2	38.9	10.9	407.7	6.5
9	30A1.2F	345.3	805.7	128.3	38.1	21.3	398.7	14.0
10	40A0F	501.1	751.7	137.1	40.7	0.0	466.1	12.5
11	40A0.6F	476.6	714.9	131.6	38.8	10.9	447.3	7.3
12	40A1.2F	454.4	681.6	126.6	37.6	21.0	430.5	10.5

FIGURES

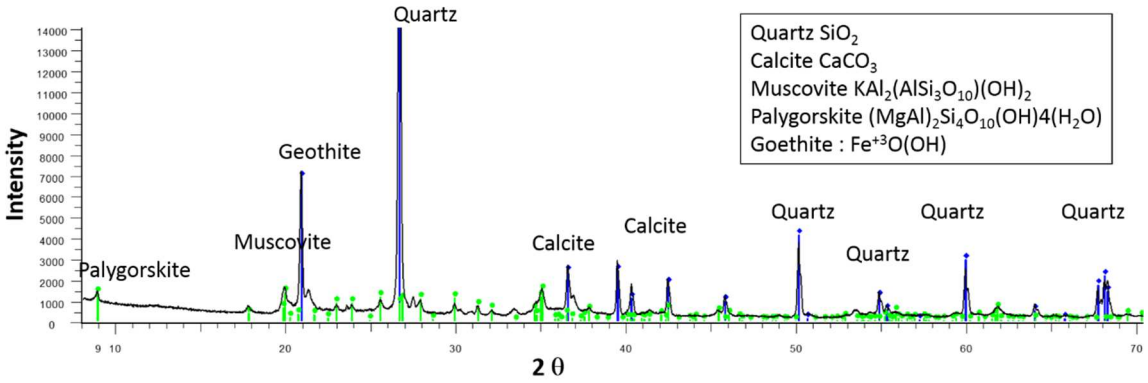

Figure 1: X-Ray Diffraction patterns of clayey soil sample

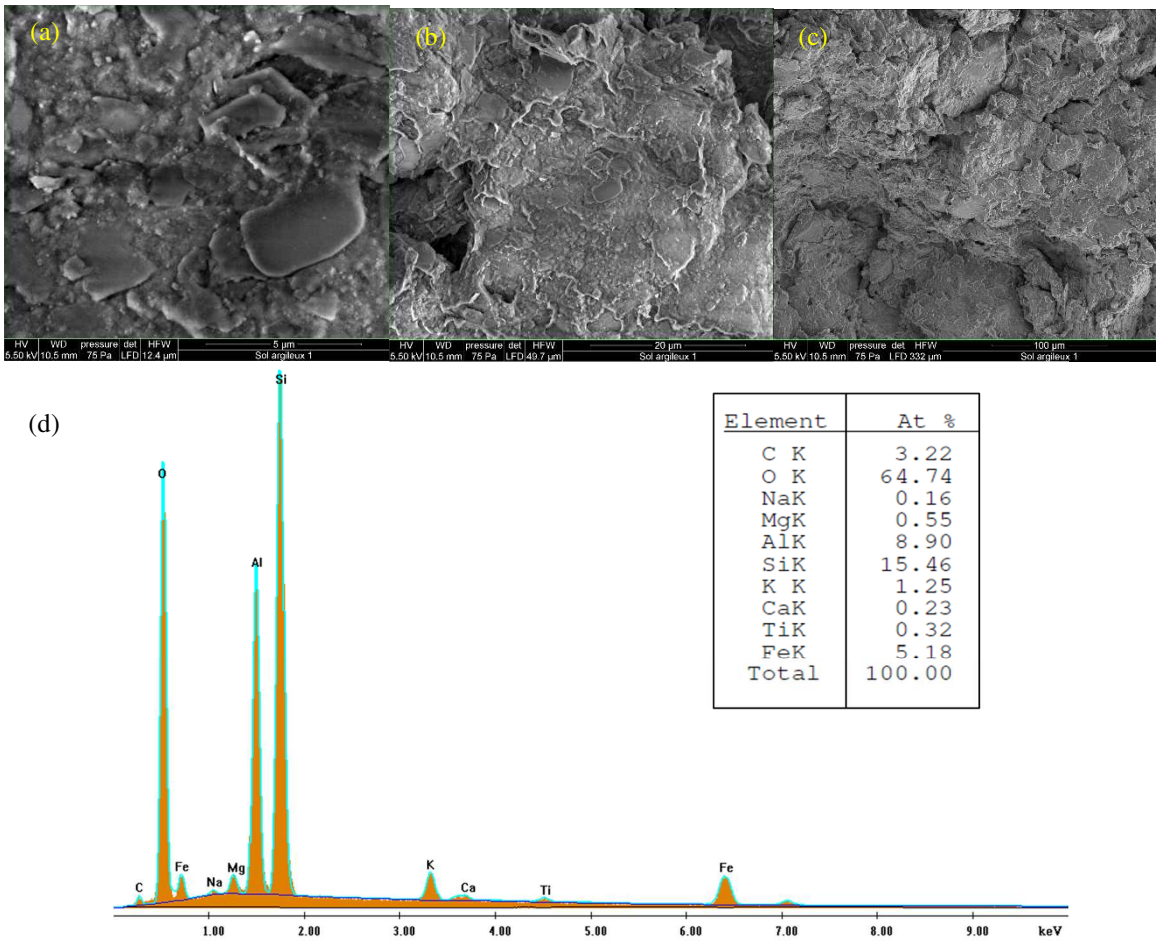

Element	At %
C K	3.22
O K	64.74
NaK	0.16
MgK	0.55
AlK	8.90
SiK	15.46
K K	1.25
CaK	0.23
TiK	0.32
FeK	5.18
Total	100.00

Figure 2: Secondary Electron (SE) high magnification image (a,b), Back Scattered Electrons (BSE) low magnification image (c) Average phase spectrum

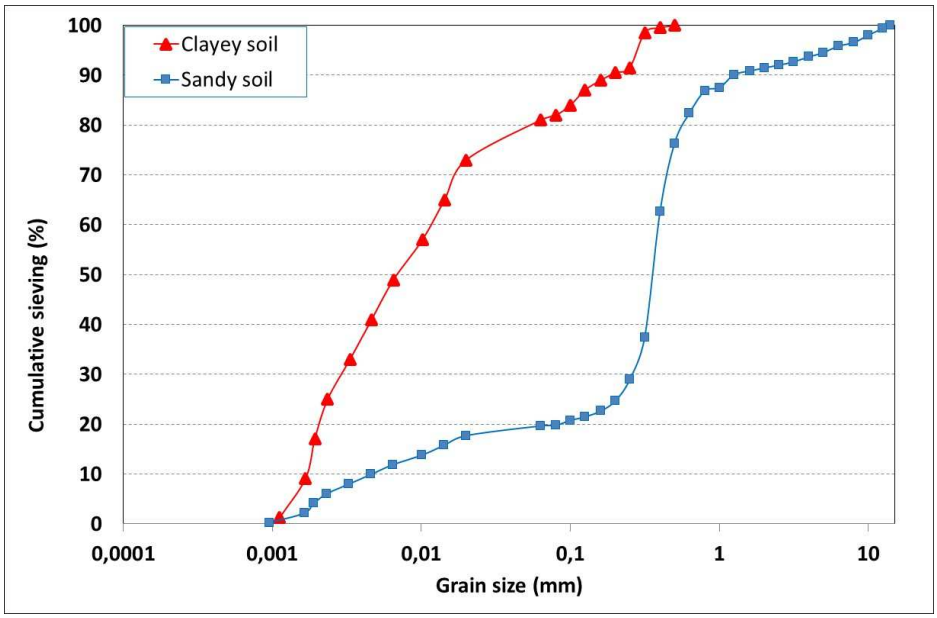

Figure 3: Grain distribution of clayey and sandy soil.

Figure 4: General view of the casted concrete, a) dry materials, b) fresh soil concrete, c) fresh concrete in cubic molds d) compressive test setup on cubic soil concrete (d)

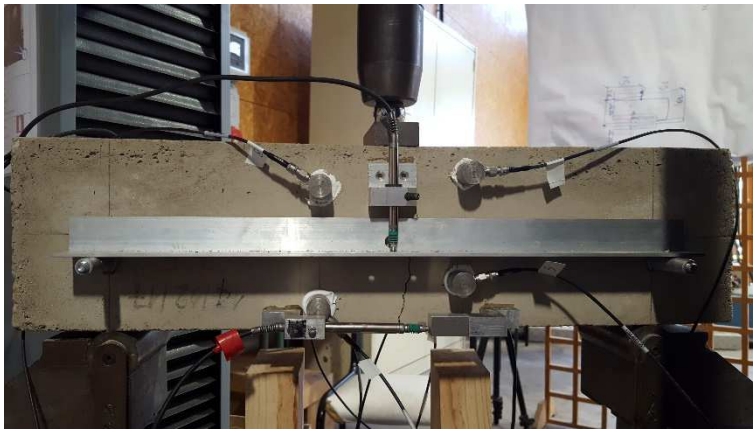

Figure 5: General view of the three-point bending test on soil concrete beams

Figure 6: Measurement of the Ultrasonic Pulse Velocity

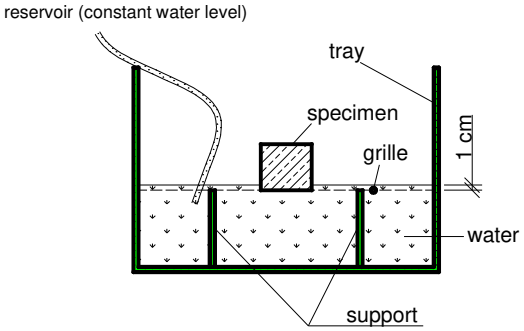

Figure 7. Schema of capillary absorption measurement

Figure 8a

Figure 8b

Figure 8 : Autogenous and drying conditions of specimens and device measurement

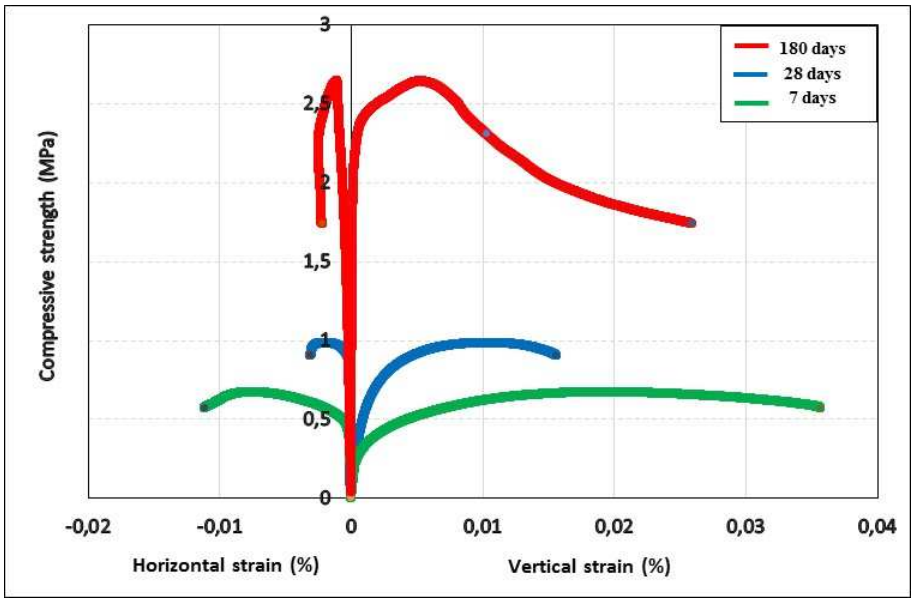

Figure 9: Compressive strength versus vertical and horizontal strain curves at 7 days, 28 days and 180 days

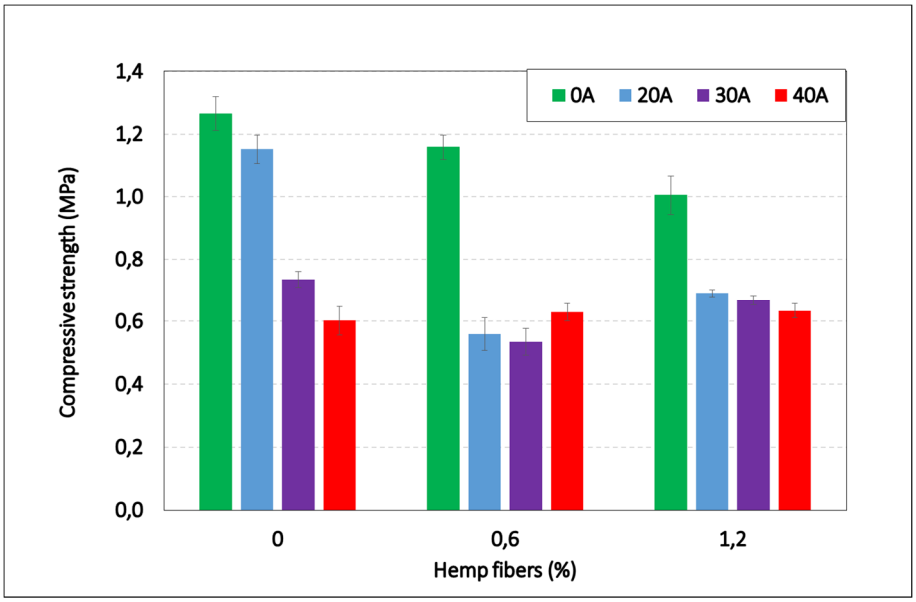

Figure 10: Effect of clayey soil and fibers on the compressive strength at 7 days.

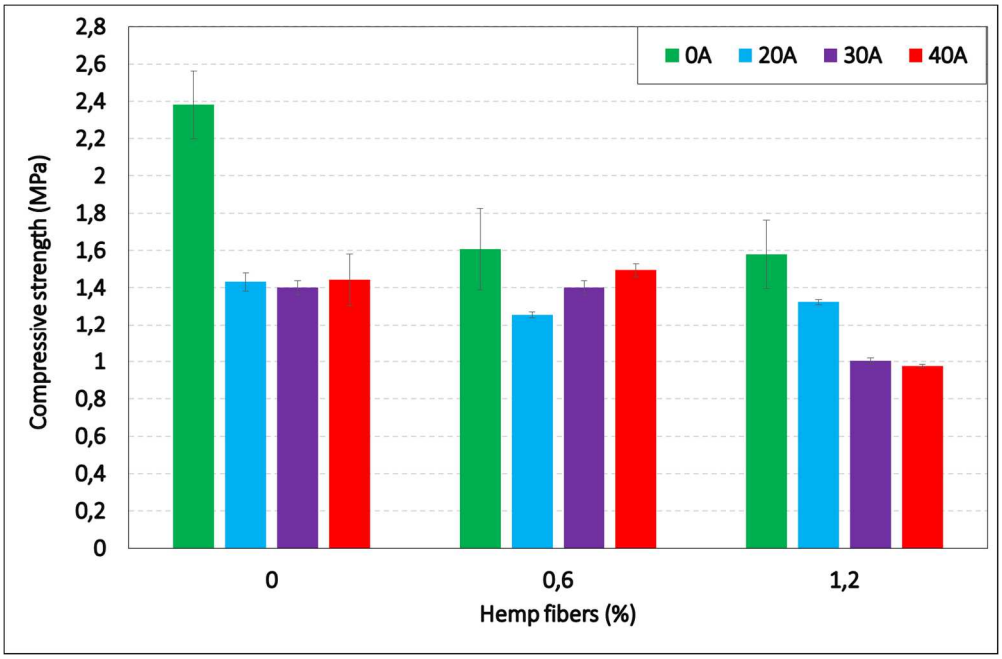

Figure 11: Effect of clayey soil and fibers on the compressive strength at 28 days.

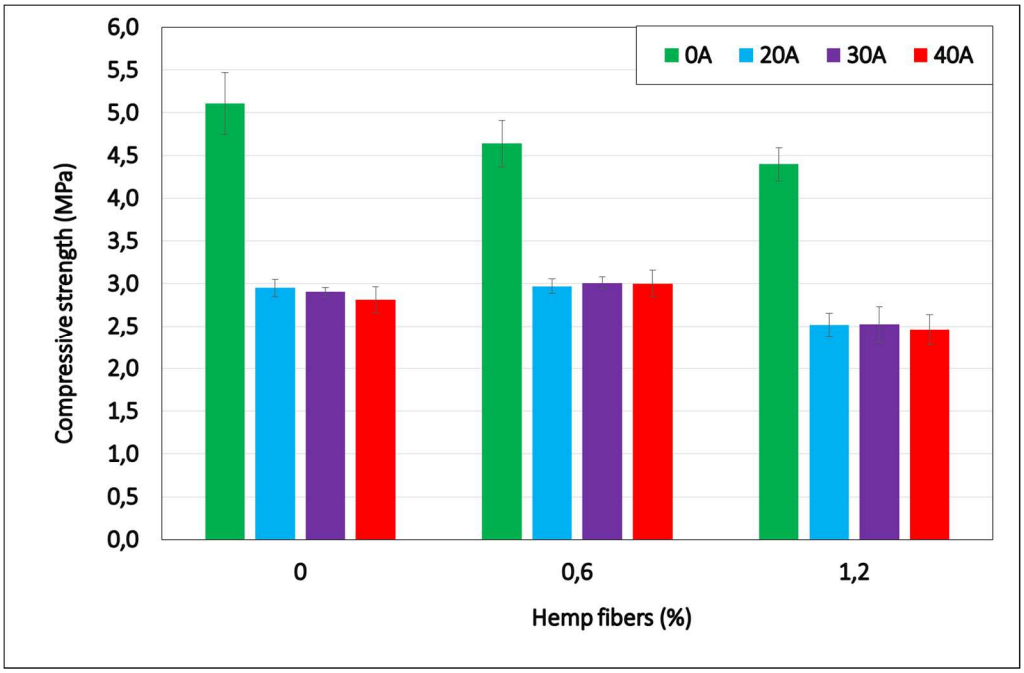

Figure 12: Effect of clayey soil and fibers on the compressive strength at 180 days.

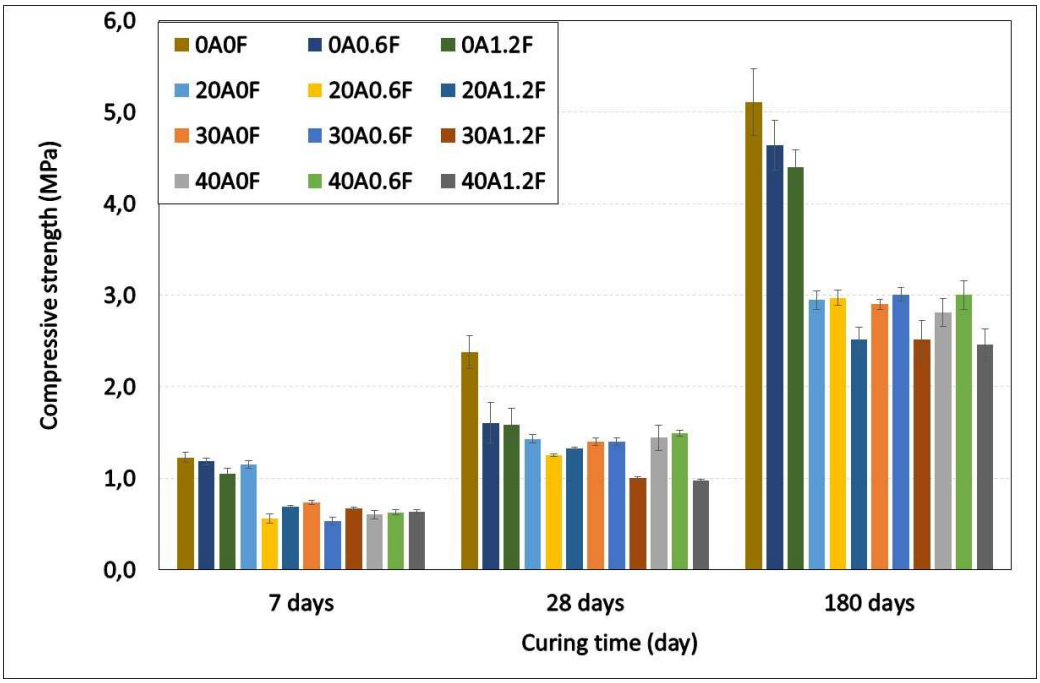

Figure 13. Compressive strength at 7, 28, and 180 days.

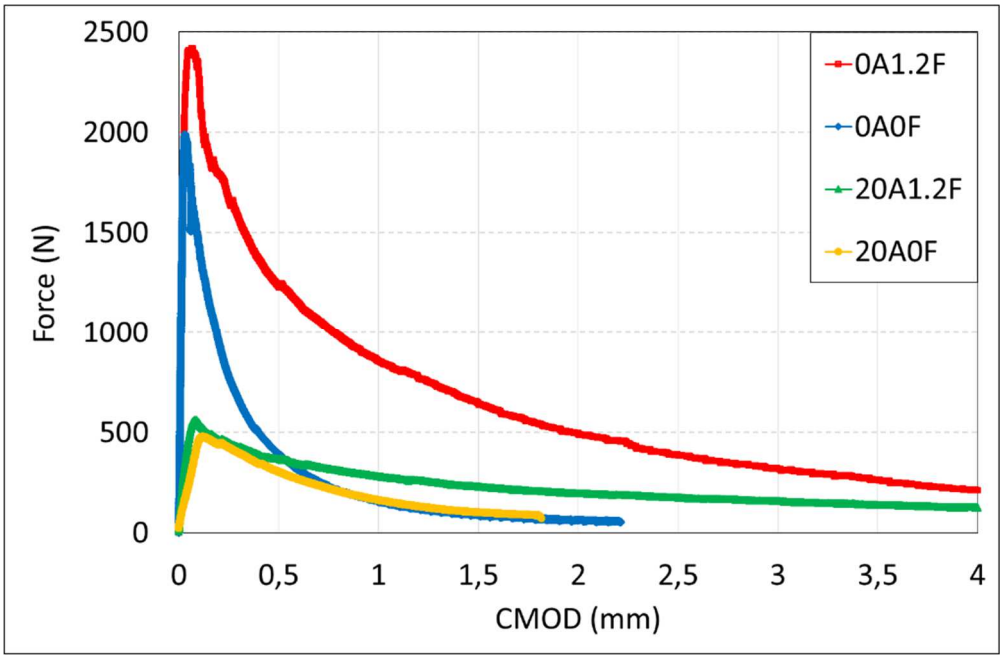

Figure 14: Influence of clayey soil and fibers on the flexural behavior

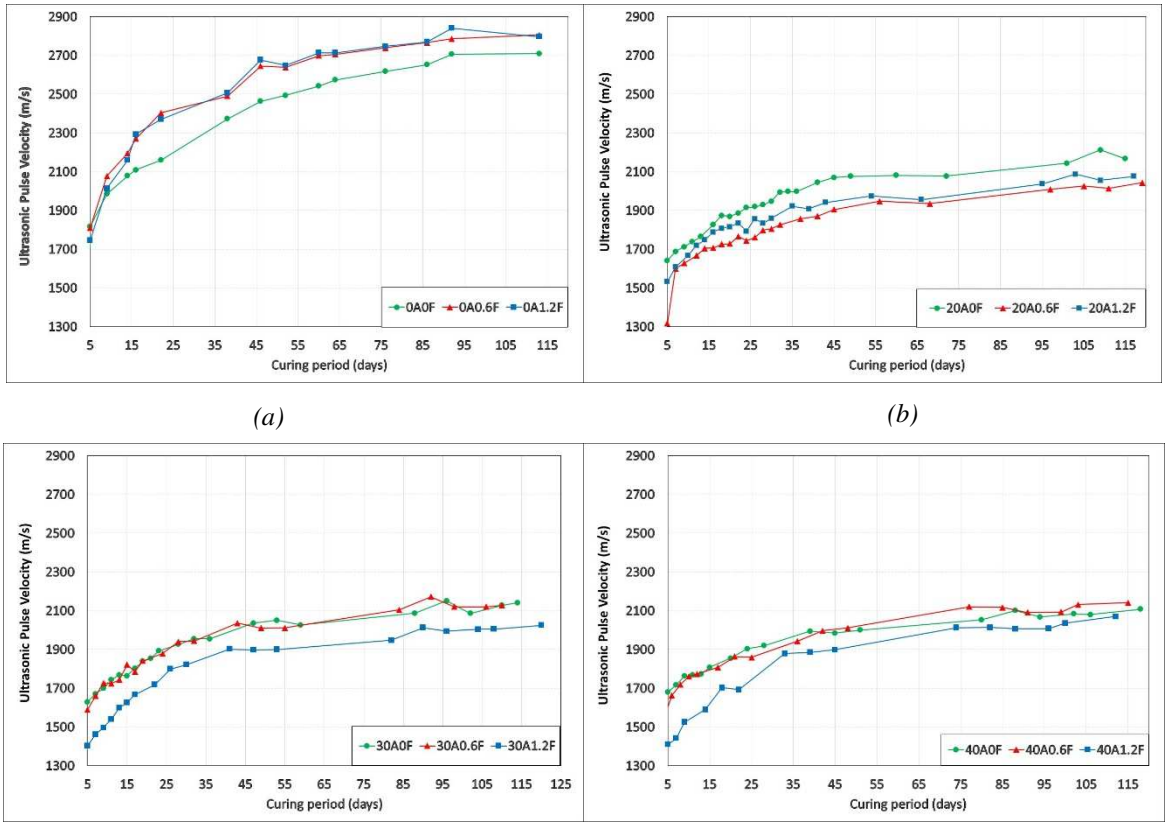

Figure 15: Influence of clayey soil and fibers on the Ultrasonic Pulse Velocity

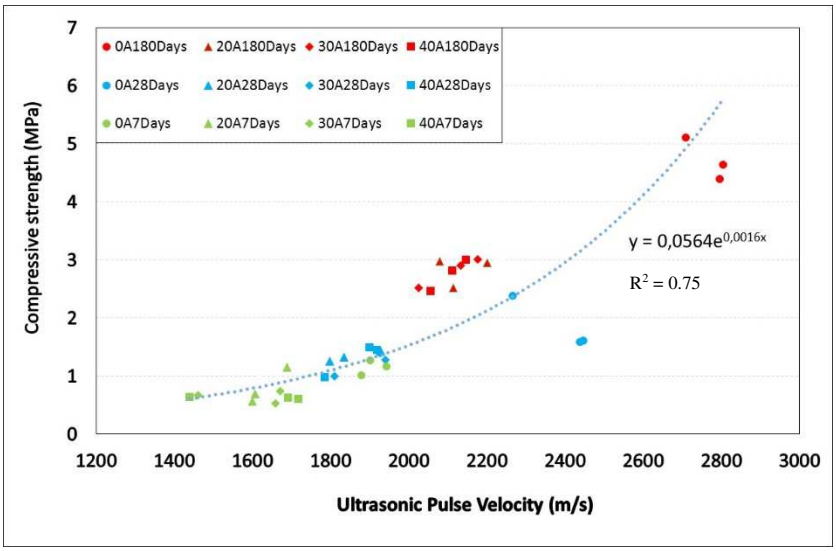

Figure 16: Correlation between Ultrasonic Pulse Velocity and compressive strength (at 7 days. 28 days and 180 days)

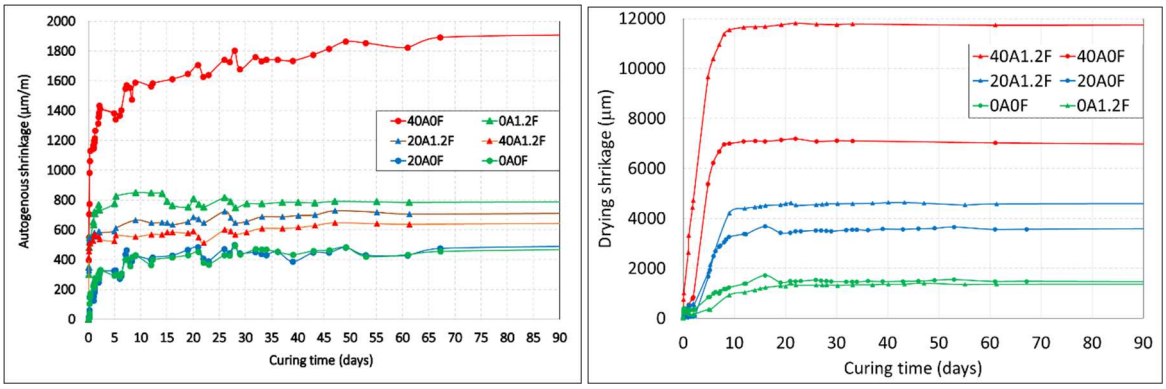

Figure 17: Influence of fibers and clayey soil on the evolution of autogenous (a) and drying shrinkage (b)

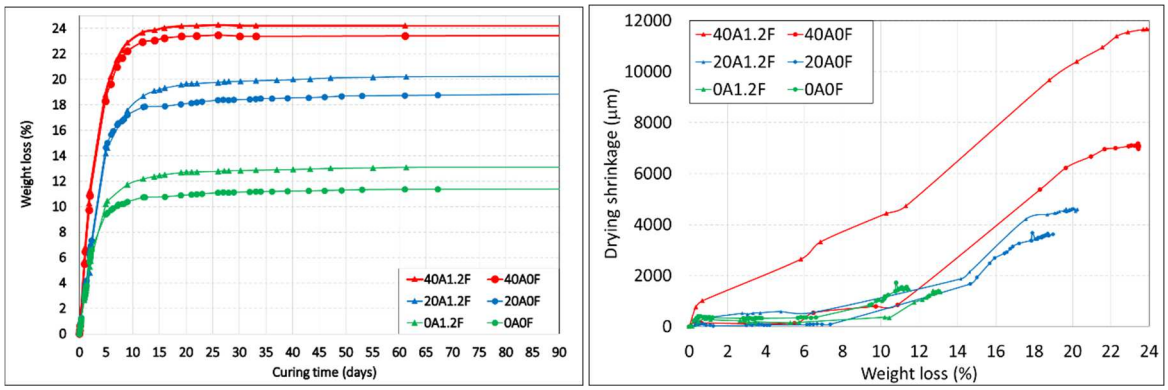

Figure 18: Evolution of the relative weight loss during drying in function of time (a) and correlation with drying shrinkage (b)

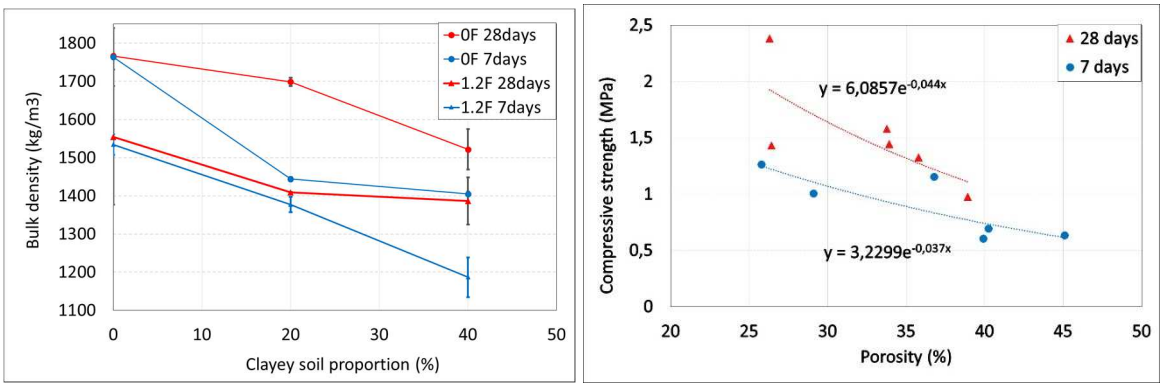

838
839
840 **Figure 19: (a) Influence of fibers and clayey soil on the bulk density, (b) correlation between**
841 **compressive strength and porosity**
842
843
844
845
846
847
848
849

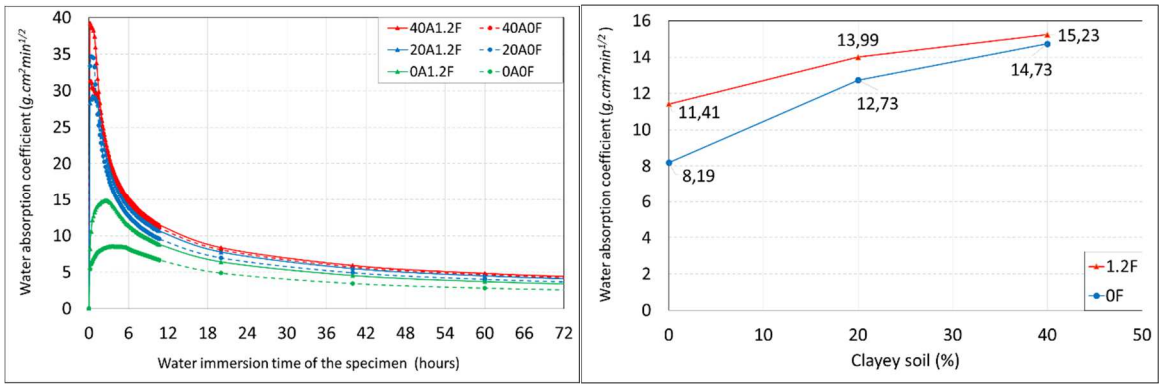

850

Fig. 20a : The evolution of water absorption coefficient *Fig. 20b : Water absorption coefficient at 6 hours*

851

852 **Figure 20: Effect of fibers and clayey soil proportions on water absorption coefficient**

Design of ecological concrete with natural soil and hemp

Local natural materials

Plastic workability

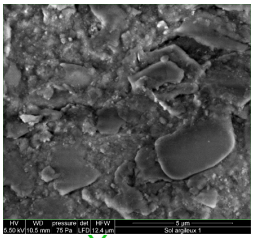

X-ray

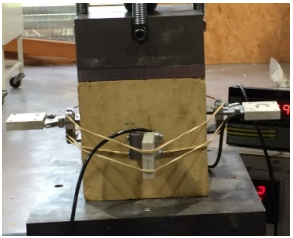

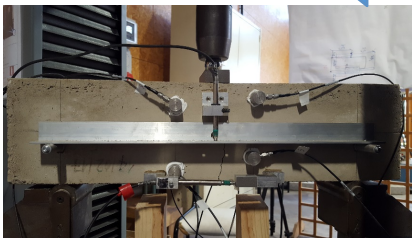

Mechanical properties and NDT testing

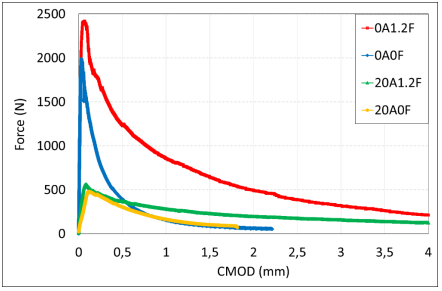

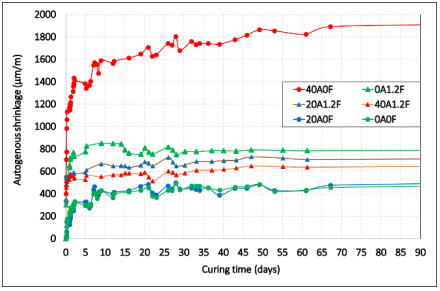

Filing concrete with interesting mechanical and physical properties with hemp incorporation